Neuron
Article

Directed Migration of Cortical Interneurons Depends on the Cell-Autonomous Action of Sip1

Veronique van den Berghe,[1] Elke Stappers,[1] Bram Vandesande,[2] Jordane Dimidschstein,[3] Roel Kroes,[1] Annick Francis,[1] Andrea Conidi,[1] Flore Lesage,[1] Ruben Dries,[1] Silvia Cazzola,[1] Geert Berx,[4,5] Nicoletta Kessaris,[6] Pierre Vanderhaeghen,[3,7] Wilfred van IJcken,[8,9] Frank G. Grosveld,[8,9] Steven Goossens,[5,10] Jody J. Haigh,[5,10] Gord Fishell,[11] André Goffinet,[12] Stein Aerts,[2] Danny Huylebroeck,[1,*] and Eve Seuntjens[1,*]
[1]Laboratory of Molecular Biology (Celgen), Department of Development and Regeneration
[2]Laboratory of Computational Biology (LCB), Center for Human Genetics (CME)
University of Leuven, 3000 Leuven, Belgium
[3]Université Libre de Bruxelles, IRIBHM (Institute for Interdisciplinary Research), and UNI (ULB Neuroscience Institute), 1070 Brussels, Belgium
[4]Unit Molecular and Cellular Oncology, VIB Department for Molecular Biomedical Research
[5]Department for Biomedical Molecular Biology
University of Gent, 9052 Gent, Belgium
[6]Wolfson Institute for Biomedical Research and Department of Cell and Developmental Biology, University College London, London WC1E 6BT, UK
[7]Welbio, Université Libre de Bruxelles (ULB), 1070 Brussels, Belgium
[8]Center for Biomics
[9]Department of Cell Biology
Erasmus MC, 3000 CA Rotterdam, the Netherlands
[10]Unit Vascular Cell Biology, VIB Department for Molecular Biomedical Research, University of Gent, 9052 Gent, Belgium
[11]NYU Neuroscience Institute, Department of Physiology and Neuroscience, New York University Langone Medical Center, New York, NY 10016, USA
[12]Developmental Neurobiology, Institute of Neuroscience, Université Catholique de Louvain UCL, 1200 Brussels, Belgium
*Correspondence: danny.huylebroeck@med.kuleuven.be (D.H.), eve.seuntjens@med.kuleuven.be (E.S.)
http://dx.doi.org/10.1016/j.neuron.2012.11.009

SUMMARY

GABAergic interneurons mainly originate in the medial ganglionic eminence (MGE) of the embryonic ventral telencephalon (VT) and migrate tangentially to the cortex, guided by membrane-bound and secreted factors. We found that Sip1 (Zfhx1b, Zeb2), a transcription factor enriched in migrating cortical interneurons, is required for their proper differentiation and correct guidance. The majority of *Sip1* knockout interneurons fail to migrate to the neocortex and stall in the VT. RNA sequencing reveals that *Sip1* knockout interneurons do not acquire a fully mature cortical interneuron identity and contain increased levels of the repulsive receptor Unc5b. Focal electroporation of Unc5b-encoding vectors in the MGE of wild-type brain slices disturbs migration to the neocortex, whereas reducing Unc5b levels in *Sip1* knockout slices and brains rescues the migration defect. Our results reveal that Sip1, through tuning of Unc5b levels, is essential for cortical interneuron guidance.

INTRODUCTION

The mammalian telencephalon is critical to higher brain functions such as processing of sensory and motor input, learning, and memory. This higher-order information processing relies on both excitatory projection neurons and inhibitory γ-aminobutyric acid (GABA)ergic interneurons, which are essential to modulate the electrical activity of the projection neurons onto which they synapse. In the cortex, interneurons comprise a minority (20%–30%) of neurons compared to excitatory neurons, but they display a remarkable diversity and can be classified based on morphological, physiological, molecular, and synaptic features (Markram et al., 2004; Ascoli et al., 2008). In mice, cortical interneurons originate in the medial and caudal ganglionic eminences (MGE and CGE) and preoptic area (POA) (Fogarty et al., 2007; Miyoshi et al., 2007, 2010; Gelman et al., 2009; Rubin et al., 2010). Besides cortical interneurons, the MGE also generates interneurons destined for the striatum and hippocampus, and oligodendrocytes and projection neurons for the globus pallidus, amygdala, and septum (Kessaris et al., 2006; Xu et al., 2008). The specification, migration, and integration of cortical interneurons are complex but precisely orchestrated processes, and disturbances in interneuron development and function have been linked to various neurodevelopmental disorders (Levitt et al., 2004).

Once specified in the ganglionic eminences, interneurons migrate to different telencephalic structures, including the neocortex. For this, they need to interpret guidance information supplied by a range of cues in the surrounding ventral telencephalon (VT). Cortical interneurons express the receptor *EphA4* and are repulsed by ephrinA5 in the ventricular zone (VZ) of the MGE and by ephrinA3 in the striatum (Zimmer et al., 2008; Rudolph et al., 2010). Neuropilin receptors (*Nrp1, Nrp2*) prevent cortical interneurons from entering the striatum, which produces the

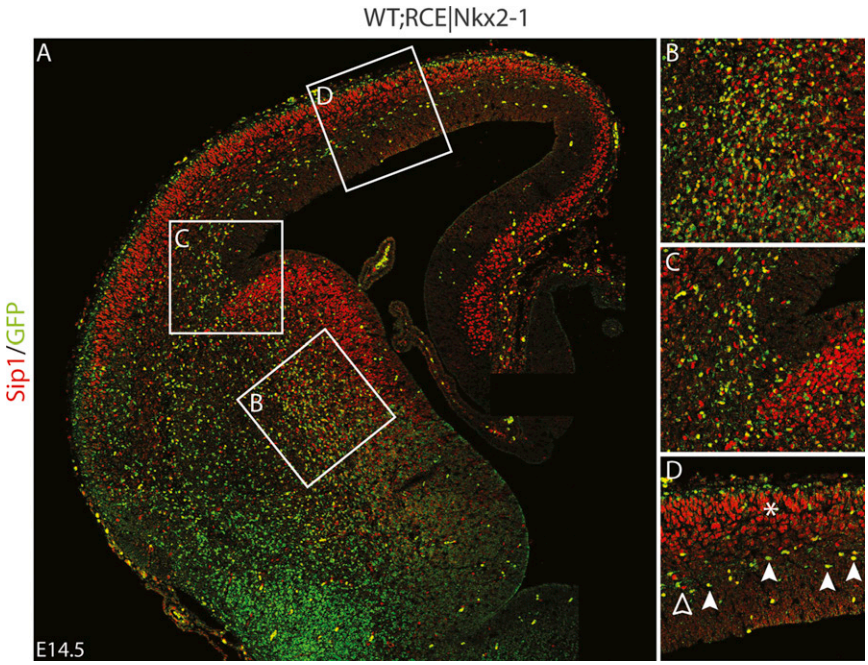

Figure 1. Sip1 Is Present in MGE-Derived Migrating Cortical Interneurons

(A) Crossing the Nkx2-1-*Cre* mouse with the RCE$^{fl/fl}$ reporter mouse labels the POA and MGE (except for the most dorsal part) and its derivatives. (B–D) Tracing experiments combined with Sip1 immunohistochemistry at E14.5 show many Sip1/GFP double-positive (+) cells migrating through the LGE (B). Many Sip1+/GFP+ cells enter the cortex (C) and are found in the SVZ/IZ (D), suggesting that these cells are MGE-derived cortical interneurons (white arrowheads, Sip1+/GFP+ cells; open arrowhead, Sip1+/GFP− cell; asterisk indicates Sip1+ cortical projection neurons).
See also Figure S1.

repulsive Sema3a and Sema3f ligands (Marín et al., 2001). Deletion of *Robo1* results in an increased influx of interneurons in the striatum and cortex (Andrews et al., 2006; Andrews et al., 2008). Robo1 interacts with Nrp1 and modulates semaphorin-neuropilin/plexin signaling to direct cortical interneurons around the striatum (Hernández-Miranda et al., 2011). Different isoforms of neuregulin-1 act as short- and long-range attractants for migrating cortical interneurons, which express the receptor gene *ErbB4* (Flames et al., 2004). Stromal-derived factor-1 (SDF1, Cxcl12) and its receptors Cxcr4 and Cxcr7 are implicated in chemotaxis and positioning of interneurons in the cortex (Stumm et al., 2003; Li et al., 2008; López-Bendito et al., 2008; Sánchez-Alcañiz et al., 2011; Wang et al., 2011).

Transcription factors are ideal candidate proteins to specify but also sort the different types of interneuron through controlling the synthesis of such guidance cues and receptors (for recent reviews, see Chédotal and Rijli, 2009; Corbin and Butt, 2011). Persistent expression of *Nkx2-1* allows a subset of MGE-derived interneurons to downregulate *Nrp2* and migrate into the striatum, whereas interneurons destined to the cortex downregulate *Nkx2-1*, maintain high Nrp2 levels, and avoid the striatum (Nóbrega-Pereira et al., 2008). However, evidence for a functional link between other transcription factors and guidance cues for migrating interneurons remains limited.

Sip1 (also named Zeb2, Zfhx1b) is a transcription factor implicated in embryonic development and in epithelial-to-mesenchymal transition (EMT) (for a recent review, see Conidi et al., 2011). Sip1 contains two clusters of zinc fingers that mediate binding to two spaced E-box sequences in regulatory regions of its target genes. Furthermore, it has domains that bind activated Smads, CtBP-1/2, and the chromatin-remodelling corepressor complex NuRD, respectively (Verschueren et al., 1999; van Grunsven et al., 2007; Verstappen et al., 2008). In humans, mutations in one *ZFHX1B* allele cause Mowat-Wilson syndrome (MWS), characterized by severe intellectual disability and typical facial features, and many patients present with seizures, corpus callosum agenesis, Hirschsprung disease, and congenital heart disease (Zweier et al., 2002; Garavelli and Mainardi, 2007).

Using various conditional knockout (KO) mice, we showed that Sip1 regulates, in a non-cell-autonomous manner, hippocampal development and the timing of cortical neurogenesis and gliogenesis (Miquelajauregui et al., 2007; Seuntjens et al., 2009). Here, using both loss- and gain-of-function approaches in vivo and ex vivo, we show that Sip1 is essential for cortical interneuron migration. Deletion of *Sip1* leads to a severe reduction in the number of interneurons in the embryonic and postnatal cortex. *Sip1* KO MGE-derived interneurons do not acquire a fully mature cortical interneuron identity, and contain increased levels of the guidance receptor Unc5b. Overexpression of Unc5b in wild-type (WT) MGE largely abrogates interneuron migration to the cortex, while reduction of Unc5b levels in *Sip1* mutant interneurons in vitro or in vivo rescues their migration defect. Thus, we discovered a role for Sip1 as a critical transcription factor regulating Unc5b mRNA levels during cortical interneuron migration.

RESULTS

Sip1 Is Abundantly Present in Migrating Cortical Interneurons

We documented the presence of Sip1 in the mouse VT by immunohistochemistry at embryonic day (E) 14.5 (Figure 1; Figure S1 available online). Sip1 is present at low levels in the VZ of the MGE and at higher levels in the mantle zone (Figures S1A, S1A′, S1B, and S1B′). In the LGE, we detected Sip1 in a sickle-shape pattern in the subventricular zone (SVZ), and in scattered Sip1-positive (+) cells in the mantle zone (Figures S1A, S1A′, S1B, and S1B′). Sip1 was also present in the CGE (Figures S1C and S1C′). Furthermore, Sip1+ cells were found across the pallial-subpallial boundary (PSB) and in the SVZ/ intermediate zone (IZ) and cortical plate (asterisk in Figure S1A).

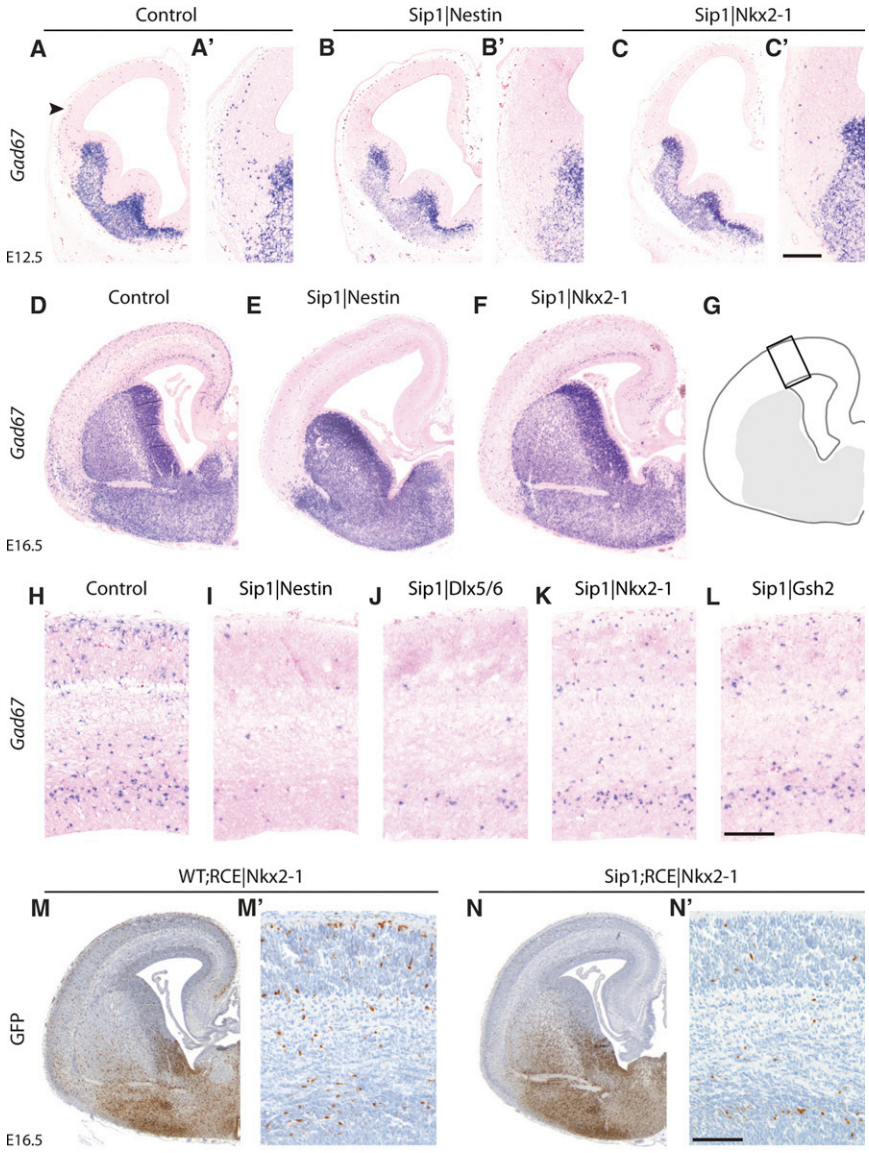

Figure 2. Hampered Tangential Migration of *Sip1* Mutant Cortical GABAergic Interneurons

(A and A′) In situ hybridization for *Gad67* mRNA at E12.5 detects GABAergic interneurons that start invading the cortical anlage in control embryos (arrowhead) (magnification in A′).

(B, B′, C, and C′) None or only few Gad67+ interneurons are detected in the cortex of Sip1|Nestin (B and B′) and Sip1|Nkx2-1 (C and C′) mutants.

(D–L) In E16.5 control embryos, GABAergic interneurons are spread throughout the cortical plate (D and magnification in H; G is a schematic representation of sections shown in D–F and indicates the area of the magnifications in H–L). In the Sip1|Nestin mutant, almost no interneurons are detected in the cortex at E16.5 (E, I). *Sip1* deletion in the MGE (Nkx2-1-*Cre*, F and K) or in the CGE, LGE, and a portion of the MGE (Gsh2-*Cre*, L) mainly reduces the number of interneurons in the cortical MZ and IZ. In the Sip1|Dlx5/6 mutant, only few interneurons are found in the cortex (J).

(M, M′, N, and N′) The RCE$^{fl/fl}$ reporter mouse line shows that the majority of the *Sip1* mutant Nkx2-1-*Cre*-derived cells (M and M′) do not migrate to the cortex when compared to a WT control (N and N′). Scale bar in (C′) corresponds to 50 μm (A′–C′), and scale bar in (L) and (N′) to 100 μm (H–L, M′, N′).

To assess whether these cells were MGE-derived interneurons destined to the cortex, we traced them by crossing the Nkx2-1-*Cre* mouse line (Kessaris et al., 2006) with RCE$^{fl/fl}$ (i.e., *R26R*$^{CAG\text{-}loxP\text{-}stop\text{-}loxP\text{-}EGFP}$) reporter mice (Sousa et al., 2009). As shown previously (Kessaris et al., 2006; Fogarty et al., 2007), cells derived from the POA and MGE, except those from its most dorsal part, were labeled. We monitored green fluorescent protein (GFP) and Sip1 in the E14.5 telencephalon (Figure 1) and confirmed that Sip1 was present at low levels in the VZ of the MGE and at increasingly higher levels in the mantle zone (Figure 1A). Most GFP+ cells migrating through the LGE contained Sip1 (Figures 1A and 1B). The majority of MGE-derived cells crossing the PSB were Sip1+ (Figure 1C) and they maintained high Sip1 levels while migrating through the neocortex (Figure 1D), demonstrating that Sip1 is present in MGE-derived migrating interneurons. Sip1+ but GFP− cells were also observed in the cortical SVZ/IZ (Figure 1C), presumably representing CGE-derived interneurons.

The Absence of Sip1 Hampers Migration of GABAergic Interneurons to the Cortex without Affecting Early Regionalization of the Ventral Telencephalon

We investigated the role of Sip1 in interneurons by removing *Sip1* using the Nestin-*Cre* mouse line (Tronche et al., 1999), which inactivates *Sip1* in the entire embryonic CNS and the Nkx2-1-*Cre* line (for details on the crossing schemes, see Supplemental Experimental Procedures). We refer to Nestin-*Cre*;*Sip1*$^{fl/KO}$ as "Sip1|Nestin" (KO) mice and to the Nestin-*Cre*; *Sip1*$^{fl/WT}$ control mice as "WT|Nestin" mice; a similar convention is used for crosses with other *Cre* lines. We confirmed Sip1 removal from the entire telencephalon in Sip1|Nestin mice (Figures S1E and S1E′), and in the POA/MGE (except its most dorsal portion) in Sip1|Nkx2-1 mutants (Figures S1F and S1F′) when compared to control mice at E12.5 (Figures S1D and S1D′).

At E12.5, when the first MGE-derived interneurons reach the dorsal telencephalon in control embryos (Figures 2A and 2A′), none or only few GABAergic interneurons (marked by Gad67) migrated in the cortical anlage of Sip1|Nestin and Sip1|Nkx2-1 mice (Figures 2B, 2B′, 2C, and 2C′). At E16.5, hardly any *Gad67*+ cells were found in the Sip1|Nestin cortex (Figures 2E and 2I; control in Figures 2D and 2H), while several were still present in the Sip1|Nkx2-1 cortex (Figures 2F and 2K), although lower in number than in controls. Those *Gad67*+ cells in the

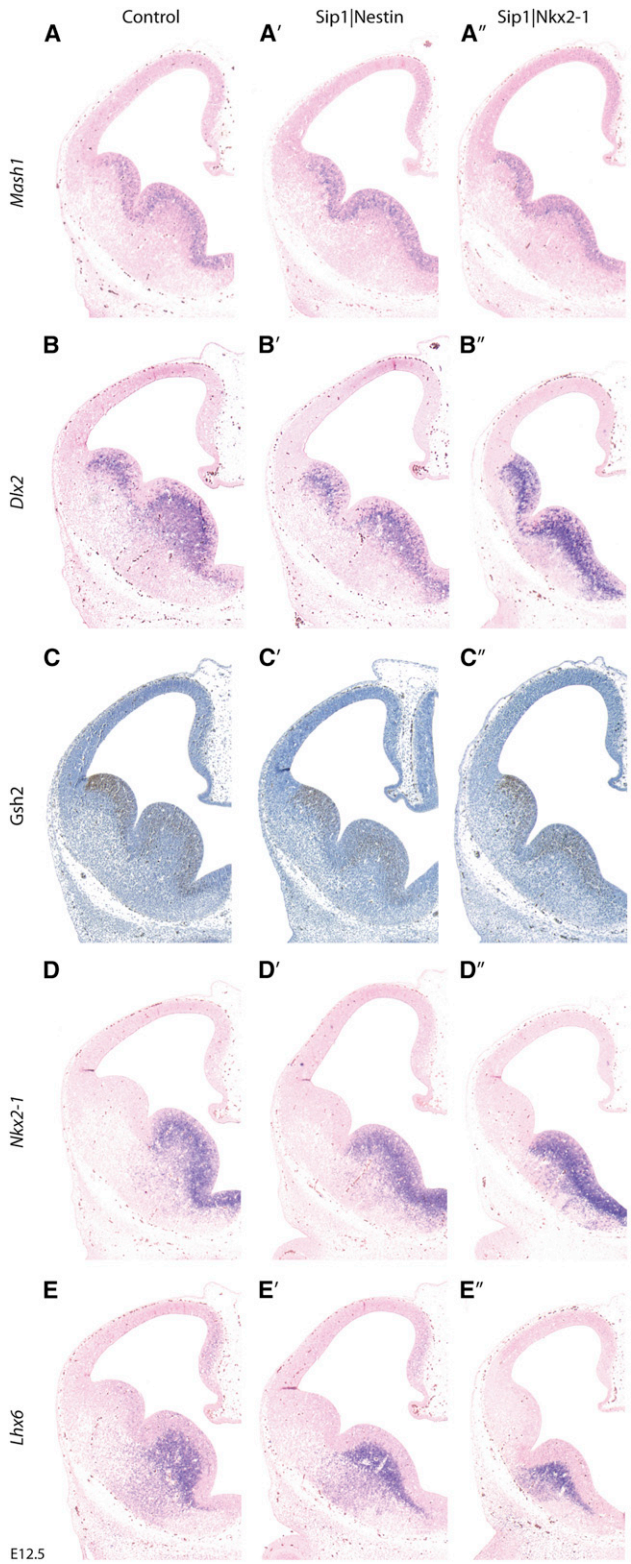

Figure 3. *Sip1* Deletion Does Not Influence Early Regionalization of the Ventral Telencephalon

(A and A′) The expression domain of *Mash1*, an important regulator of neurogenesis, is unchanged upon *Sip1* deletion.

(B and B′) *Dlx2* is expressed in the ganglionic eminences (MGE, LGE, and CGE), and its expression is not changed in the Sip1|Nkx2-1 and Sip1|Nestin mutants at E12.5.

(C and C′) Gsh2 marks the LGE and CGE, but also to a lesser extent the MGE. Gsh2 levels are not changed in the MGE of *Sip1* mutants, suggesting that the MGE does not adopt an LGE or CGE identity.

(D and D′) Expression of *Nkx2-1* is not affected in *Sip1* mutants.

(E and E′) *Lhx6*, a direct target gene of Nkx2-1, was also correctly expressed in the *Sip1* mutants at E12.5.

Sip1|Nkx2-1 mutant cortex might have originated from the untargeted CGE. Lineage tracing with the RCE$^{fl/fl}$ reporter in the Nkx2-1 model confirmed that the migration of MGE-derived cells to the cortex was severely compromised in the absence of Sip1 (Figures 2M, 2M′, 2N, and 2N′).

We substantiated these observations using two additional *Cre* mouse lines: Dlx5/6-*Cre*, which targets the entire VT, except its VZ (Stenman et al., 2003), and Gsh2-*Cre,* which produces Cre in the LGE, CGE, and a portion of the MGE (Kessaris et al., 2006). Both Sip1|Dlx5/6 and Sip1|Gsh2 brains had reduced numbers of *Gad67*+ cells in the cortex, comparable to those found in Sip1|Nestin and Sip1|Nkx2-1 mutants, respectively (Figures 2J and 2K). In contrast to Sip1|Dlx5/6 and Sip1|Nestin mice, which die at birth, Sip1|Nkx2-1 and Sip1|Gsh2 mice are viable. Interestingly, in the latter animals, we occasionally observed myoclonic seizures during the third postnatal week.

Next, we assessed whether the lack of Sip1 modified the expression of acknowledged MGE/VT markers. We performed in situ hybridization for *Mash1*, *Dlx2*, *Nkx2-1*, and *Lhx6,* and immunohistochemistry for Gsh2 in E12.5 control and KO sections. At this stage, all markers were still present in their appropriate domains in Sip1|Nestin and Sip1|Nkx2-1 embryos (Figures 3A–3E), suggesting that deletion of *Sip1* did not affect early regionalization of the VT.

Defective Migration of *Sip1*-Deleted Cortical Interneurons Is Due to Removal of Cell-Autonomous Effects of Sip1

In the cortex, Sip1 controls a non-cell-autonomous feedback mechanism that emanates from Sip1+ postmitotic neurons to progenitor cells, thereby timing neurogenesis and gliogenesis (Seuntjens et al., 2009). We therefore investigated whether the action of Sip1 in the MGE would be cell autonomous or not. We performed focal electroporations (Figure 4A) with *Cre* plasmid pCIG-*Cre* in the MGE of E13.5 *Sip1*$^{fl/fl}$ organotypic brain slices (Figures 4D and 4D′). After 3 days in vitro (DIV), we counted the total number of GFP+ cells in the slice and calculated the percentage of GFP+ neurons that reached the cortex. As controls, we electroporated pCIG-*Cre* in WT slices or a GFP-encoding plasmid (pCIG) in *Sip1*$^{fl/fl}$ slices (Figures 4B, 4B′, 4C, and 4C′). In both controls, targeted GFP+ cells migrated to the cortex (58.3% for pCIG in *Sip1*$^{fl/fl}$ slices, n = 11; 56.8% for pCIG-*Cre* in WT slices, n = 13 slices; quantification in E). By contrast, only 14% of the *Sip1*-deleted cells (pCIG-*Cre* in *Sip1*$^{fl/fl}$ slices, n = 19 slices, $p < 0.001$; two independent experiments) migrated to the cortex (Figures 4D and 4E).

The failure of the neighboring Sip1+ cells to rescue the defective tangential migration of *Sip1* mutant interneurons

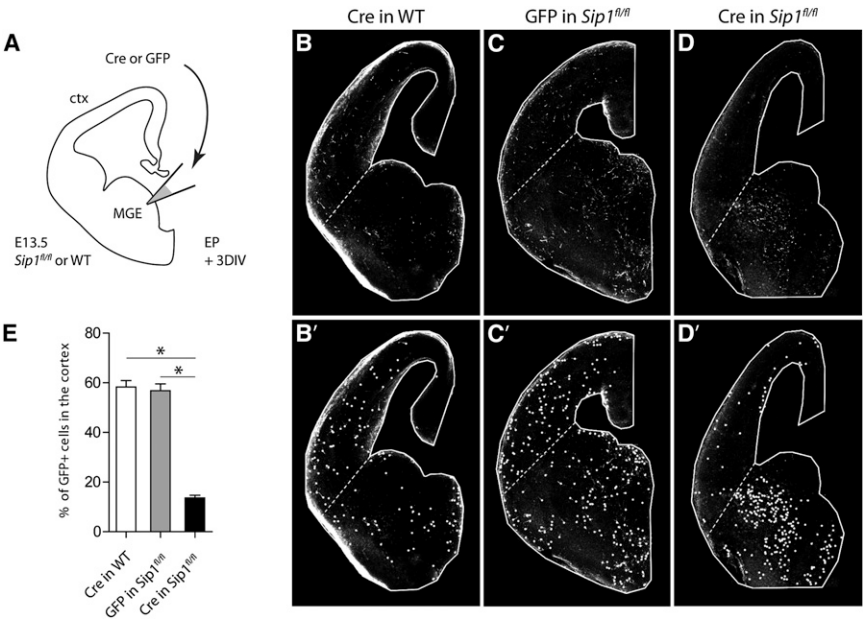

Figure 4. Sip1 Has a Cell-Autonomous Role in Cortical Interneurons

(A) Experimental design to delete *Sip1* in a limited number of MGE cells. pCIG (pCAGGS-IRES-*eGFP*) or pCIG-*Cre* plasmids were focally electroporated (EP) in the MGE of *Sip1*$^{fl/fl}$ E13.5 organotypic brain slices and cultured for 3 DIV. To check for a possible toxic effect caused by Cre accumulation, the pCIG-*Cre* construct was electroporated in WT slices.

(B–D) Representative pictures of each experimental condition. The border between cortex and VT is indicated by the dotted line. Lower panels (B′–D′) with digitally added dots indicate the counted GFP+ cells.

(E) We counted the total number of GFP+ cells per slice and calculated the percentage of GFP+ neurons in the cortex. Electroporation of pCIG-*Cre* in WT MGE or pCIG in *Sip1*$^{fl/fl}$ MGE resulted in similar proportions of targeted cells in the cortex (58.28% ± 2.61%, n = 11 slices and 56.83% ± 2.74%, n = 13 slices, respectively). Migration to the cortex of Sip1-deficient interneurons is strongly decreased (13.63% ± 1.07%, n=19) compared to both controls. Error bars represent SEM of two independent experiments. Statistical significance was determined using the χ^2 test (*p < 0.001).

demonstrated that the effects of Sip1 in interneuron migration are cell autonomous.

Sip1-Deficient Interneurons Are Intrinsically Able to Migrate

We next investigated whether Sip1-deficient cells had the intrinsic capacity to migrate. We cultured MGE explants from WT;- and Sip1;RCE|Nkx2-1 E14.5 embryos in Matrigel (Figure S2A) according to (Wichterle et al., 1999) and measured the maximum migration distance of the cells from the explants after 1 and 2 DIV (Figures S2B and S2B′). *Sip1* KO interneurons migrated about 15% less far from the explants than WT counterparts after 1 DIV (WT: 252.95 ± 13.70 μm, n = 29 versus KO: 215.77 ± 15.41 μm, n = 27; p = 0.0530; n = number of explants) or 2 DIV (WT: 685.06 ± 33.82 μm, n = 17 versus KO: 579.84 ± 22.68 μm, n = 21; * p = 0.0076) (Figure S2C), suggesting reduced migration speed. If the latter would be the sole cause of the observed reduction in interneuron numbers in the cortex of *Sip1* KO embryos, then the defect could be restored at later stages, when all targeted cells had sufficient time to populate the cortex. However, in Sip1;RCE|Nkx2-1 mutants, only a few GFP+ cells were found in the cortex at later stages (E18.5; Figures S2D and S2E).

A large group of misrouted *Sip1* KO cells was found in the caudal VT of Sip1;RCE|Nkx2-1 brains at E16.5 (Figures 5A, 5A′, S3A, and S3A″). This ectopic group of cells was positive for *Nkx2-1* (Figures 5B and 5B′) and *Lhx6* (Figures 5C and 5C′). Similar ectopia were found in the other *Sip1* mutants (Sip1|Nestin [see Figures 5 and S3]; Sip1|Dlx5/6 and Sip1|Gsh2 [data not shown]). These GFP+ ectopic cells did not locate to the globus pallidus (GP) area; also, they were *Er81*$^{-}$ indicating this is not an ectopic GP (Figures S3A and S3A″, where GP is indicated by an asterisk and ectopic cells by an arrowhead; results not shown). The ectopia was also positive for neuropeptide-Y (NPY), somatostatin (Sst), and *Sox6* (Figures 5D and 5E, and data not shown), as well as for receptors typically present in migrating cortical interneurons, such as *Nrp2* and *ErbB4*, indicating cortical interneuron features (Figure S3, all panels B and C).

We investigated whether Sip1;RCE|Nkx2-1 cells present in the cortex 3 weeks after birth contributed to the cortical interneuron lineages. Quantification of the number of GFP+ cells in the cortex showed there were much less MGE-derived interneurons in the *Sip1* mutants (48% of the control number) (Figure 6E). Furthermore, *Sip1* KO cells largely failed to populate the more medial parts of the cortex and remained clustered in the lateral cortex (KO versus control in lateral, 60.4% compared to 35.8% of the total population of GFP+ cells for each genotype (i.e., 61 compared to 75 cells); intermediate, 25.5% compared to 37.2% [i.e., 26 compared to 78 cells]; and medial, 14.1% compared to 27.0% [i.e., 14 compared to 56 cells]; Figures 6A–6C, 6A′–6C′, 6D, 6E, S4A, S4B, and S4E). Interestingly, the deep layers (marked by Ctip2) seemed to contain fewer GFP+ neurons when compared to control mice (Figures 6A–6C, 6A′–6C′, S4A, and S4B). We also analyzed the expression of parvalbumin (PV), Sst, calretinin (CR), and NPY in *Sip1*-deleted cortical interneurons. Most of the WT;RCE|Nkx2-1 cells in the cortex were PV+ or SST+ interneurons, less were NPY+, and almost none contained CR, as expected for MGE-derived cells (Figures 6F–6I, quantification in 6J and 6K). We found significantly fewer PV-, SST-, and NPY-containing interneurons in the cortex of Sip1;RCE|Nkx2-1 mutants (absolute numbers, p < 0.0001 for PV and SST, p = 0.0128 for NPY) (Figures 6F′-6I′, and 6J). Interestingly, the relative contribution of each of these interneuron subtypes to the total amount of targeted (GFP+) cells was not changed compared to control mice (Figure 6K).

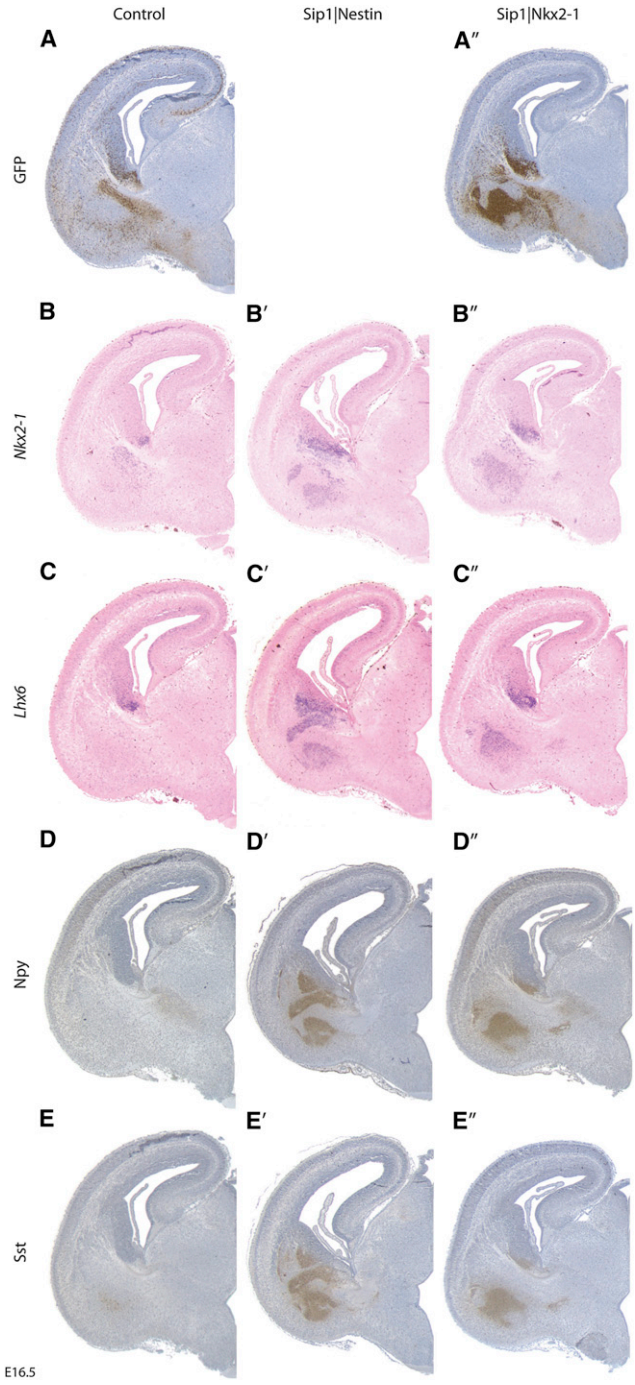

Figure 5. MGE-Derived Cells Form an Ectopia in the Caudal Part of the *Sip1* Mutant Ventral Telencephalon

(A and A′) *Sip1* KO MGE-derived cells migrate but locate in a caudal ectopia in the VT as marked by GFP+ staining in Sip1;RCE|Nkx2-1 brains (E16.5).

(B and B′, C and C′) *Nkx2-1* and *Lhx6* are also found in this ectopic cell population of all *Sip1* mutant embryos (Sip1|Gsh2 and Sip1|Dlx5/6 mutants not shown). In *Sip1* mutants, *Nkx2-1* and *Lhx6* mRNA domains in the caudal MGE are expanded.

(D, D′, E, and E′) The ectopic cells are also positive for neuropeptide Y (Npy) and somatostatin (Sst), markers of subsets of MGE-derived interneurons.

See also Figures S2 and S3.

Taken together, *Sip1* KO MGE-derived interneurons have the intrinsic capacity to migrate, yet largely fail to reach the cortex during embryogenesis. Instead, a large portion appears to be misrouted in the VT, indicating a guidance problem. Three weeks after birth, the small number of *Sip1* KO interneurons in the cortex do not distribute properly, yet still contribute to the different interneuron subtypes.

RNA Sequencing Reveals that Transcript Levels of Differentiation Factors and Guidance Cues Are Affected in *Sip1* Mutant Interneurons

To further characterize the nature of the *Sip1* KO cells and to understand the cause of the misrouting, we compared control and *Sip1* mutant transcriptomes via RNA sequencing (RNA-seq) of fluorescence-activated cell sorting (FACS) sorted MGE-derived cells, obtained from WT;- and Sip1;RCE|Nkx2-1 telencephali (three biological repeats, Illumina HiSeq-2000 platform), respectively. This approach identified differentially expressed genes irrespective of the cells' position in the telencephalon.

Gene expression levels were derived from the read counts via HT-Seq and normalized across the six samples using DE-Seq (false discovery rate [FDR] < 0.05 cutoff) (Anders and Huber, 2010). Hence, the obtained values are normalized mean read counts allowing direct comparison of control and mutant samples. We assessed the correlation among the three biological repeats (Figure S5A). The control samples and the KO samples clustered in two highly different groups, indicating that the expression differences in our samples reflected changes caused by *Sip1* deletion. A principal component analysis showed grouping of the samples according to the most important first principal component (Figure S5B). The drastic decrease of mapped reads on the floxed exon7 confirmed the efficiency of *Sip1* deletion (Figure S5C). Differential expression analysis using HT-Seq and DE-Seq identified 505 significantly upregulated and 366 significantly downregulated genes in Sip1;RCE|Nkx2-1 compared to control cells (Table S7).

To study the impact of *Sip1* deletion on differentiation of MGE-derived cell populations, we listed the expression differences of transcription factors (TFs) related to these populations in control versus *Sip1* KO cells (Table S1). We found that transcript levels of *Dlx1, Dlx2,* and *Lhx6* were not affected. Some TFs present in cortical interneurons (*Cux2*, *Maf*, and *Mafb*) were clearly reduced (gray overstrike when > 2-fold reduction), whereas others (*Satb1* and *Sox6*) were not changed or even increased. Also, the transcript levels for oligodendrocyte TFs *Olig1*, *Olig2*, and *Sox10* were downregulated, whereas *Id4*, an inhibitor of oligodendrocyte differentiation, was upregulated in the absence of Sip1. Some TFs related to striatal (*Nkx2-1*), cholinergic (*Lhx8* and *Isl1*), or pallidal (*Gbx1*) development were increased in *Sip1* KO, but none exceeded 2-fold upregulation. Furthermore, we compared the mRNA levels of 11 additional genes (*Cxcr4*, *Gria1*, *Ets1*, *Cxcr7*, *Grik1*, *Cntnap4*, *Grip1*, *Chl1*, *Cacng2*, *Csdc2*, and *Scn1a*) previously reported as enriched in embryonic cortical interneurons (Batista-Brito et al., 2008; Marsh et al., 2008; Faux et al., 2010) and included *Nrp2*, a gene related to migration of cortical interneurons (Nóbrega-Pereira et al., 2008). In the *Sip1* KO samples, 10 of these 11 genes were downregulated, whereas *Nrp2* was upregulated. Most of the

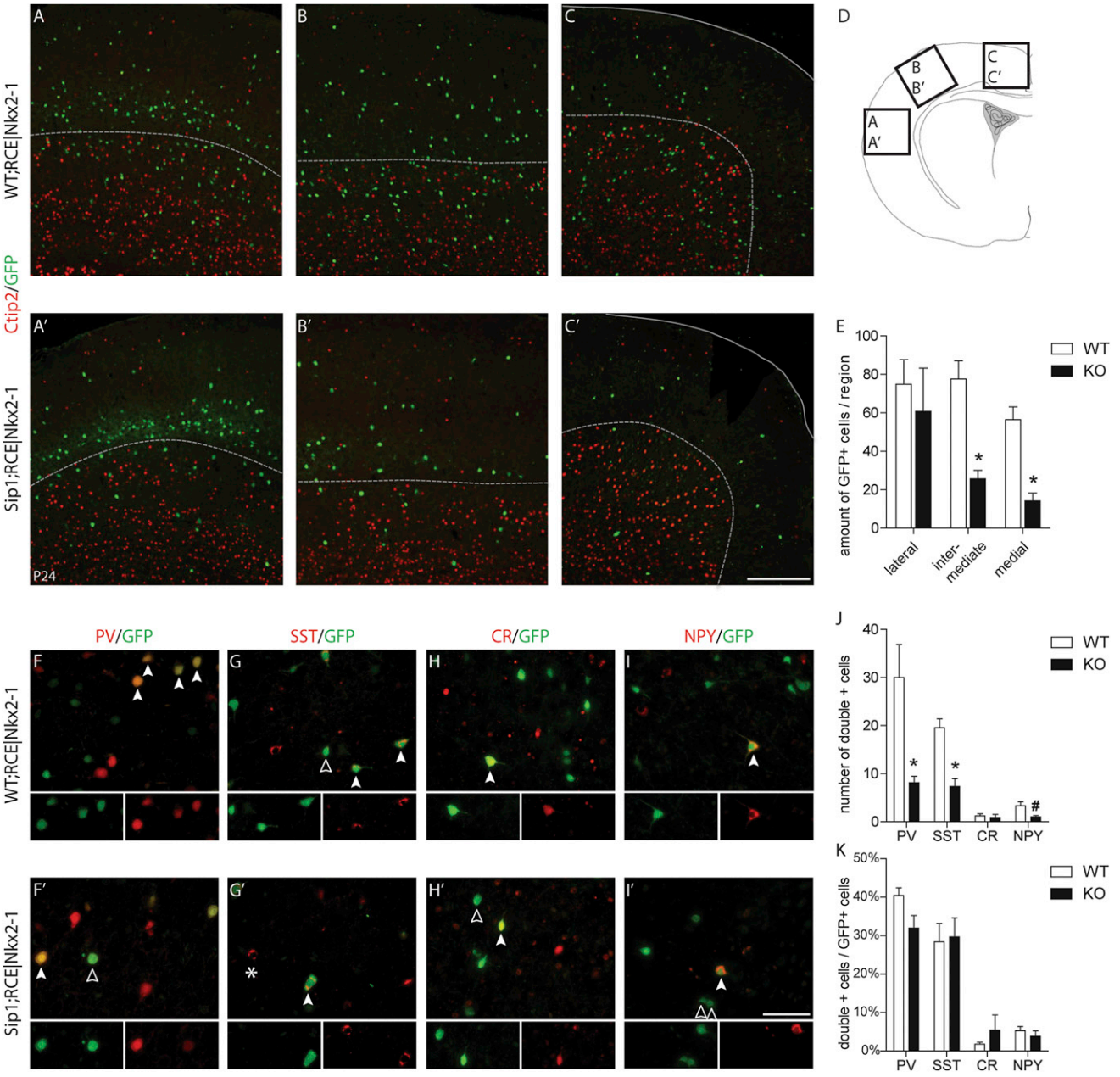

Figure 6. *Sip1* Mutant Cells Distribute Abnormally in the Postnatal Cortex but Still Contribute to the Different Interneuron Populations

(A–C and A′–C′) Three weeks after birth, few MGE-derived interneurons are found in the cortex of Sip1;RCE|Nkx2-1 mice. Compared to the control (A–C), the bulk of *Sip1* KO cells remains in the lateral cortex (A′), while only a minority are found in more medial regions (B′ and C′).

(D) Boxed areas represent the three cortical regions in the pictures in A, A′ to C, C′.

(E) Quantification of the absolute number of GFP+ cells in each of these regions shows a significant reduction in the intermediate and medial areas (KO versus control in lateral, 61 compared to 75 cells; intermediate, 26 compared to 78 cells; and medial areas, 14 compared to 56 cells).

(F–I and F′–I′) Coexpression of GFP with the interneuron markers PV, SST, CR, and NPY was compared between WT;RCE|Nkx2-1 (F–I) and Sip1;RCE|Nkx2-1 (F′–I′). White arrowheads indicate double-positive cells, empty arrowheads point to GFP+/marker− cells and an asterisk marks GFP− interneurons. Green and red channels are shown for the indicated cells.

(J) The absolute number of GFP/marker double-positive cells was significantly decreased in the *Sip1* mutant (KO versus control for PV, 8 compared to 30 cells; SST, 7 compared to 20 cells; NPY, 1 compared to 3 cells) except for CR (KO versus control for CR, 1 compared to 1 cell).

(K) The relative contribution of each of the different MGE-derived cell types was not changed (KO versus control for PV, 32% compared to 40%; SST, 30% compared to 28%; CR, 25% compared to 2%; NPY, 4% compared to 5%).

Scale bar in C′ is 250 μm (A, A′ to C, C′) and 50 μm in I′ (F, F′ to I, I′). Error bars represent SD. Statistical significance was determined via the Student's t-test ($^{*}p < 0.0001$, $^{\#}p < 0.05$).

See also Figure S4.

downregulated genes are related to interneuron function or migration in the cortex itself, suggesting that *Sip1* deletion disturbed the maturation of MGE-derived cells to functional cortical interneurons.

Next, we performed an unbiased gene ontology (GO) enrichment analysis using the GOrilla tool (http://cbl-gorilla.cs.technion.ac.il) (Tables S2 and S3). Genes related to the GO terms ''cell cycle'' and ''mitosis'' were enriched among the downregulated genes (Table S2). However, although proliferation at E12.5 in the MGE of Sip1|Nestin animals was decreased by 25% (n = 5 for each condition, p = 0.0023), cell cycle exit was not affected and we could not detect a similar reduction in proliferation in Sip1|Nkx2-1 animals (data not shown). On the other hand, genes related to ''axon guidance'' were enriched (to a factor 6.5; Table S3) among the most upregulated genes in the *Sip1* mutants. As predicted from our observed cell-autonomous action mode of Sip1, their gene products localized preferentially to the membrane and were implicated in ''signaling by transmembrane receptors'' (Table S3). Intriguingly, all four genes relating to the GO term ''Netrin receptor activity'' (i.e., *Deleted-in-colorectal-carcinoma* [*Dcc*], *Unc5a*, *Unc5b,* and *Unc5c*) were ranked within the first 294 of all 8,485 genes listed (Enrichment = 28.86; p = 3.76E-6). In fact, many of the ligands or receptors involved in the Netrin/Unc5 pathway had upregulated expression in *Sip1* KO cells (Figure S6A). Transcripts encoding the Netrin1 receptor *Unc5b* (5.3-fold up) and the ligand *Netrin1* (*Ntn1*) itself (2.4-fold up) were particularly increased (Figure S6A), which was confirmed by quantitative PCR (qPCR) (Figure S6B).

Taken together, E14.5 *Sip1* KO cells downregulate markers of maturing cortical interneurons, and possess disturbed levels of guidance cues, especially those related to Netrin/Unc5 signaling.

Increased *Unc5b* Levels Lead to Aberrant Interneuron Migration

We examined the expression of several receptors and ligands of the Netrin/Unc5 system. Unc5b mRNA was barely detectable in the control MGE, whereas *Unc5b*+ cells accumulated in the Sip1;RCE|Nkx2-1 MGE (Figures 7A, 7A′, 7B, and 7B′). *Ntn1* levels were increased around the striatal area as well as in the caudal ectopia (Figures S6C and S6C′). *Unc5c* levels increased in the VT of *Sip1* mutants, whereas *Dcc* expression was unchanged (Figures S6D, S6E–D ′, and S6E′). The fibronectin and leucine-rich transmembrane proteins Flrt2 and Flrt3 are also ligands for Unc5b (Karaulanov et al., 2009; Yamagishi et al., 2011). *Flrt2* was abundant in the LGE and striatal anlage in control and Sip1|Nkx2-1 telencephalon (Figures S6F and S6F′), whereas *Flrt3,* present at the border between the LGE and the MGE and at low level in the MGE in the control, seemed to be expanded in the mutant VT (Figures S6G–S6G′). Taken together, both qPCR and in situ hybridization analysis confirmed the increased transcript levels of *Unc5b* and *Ntn1* found by RNA-seq in Sip1;RCE|Nkx2-1 cells.

To test which candidate cue(s) is (are) likely to (mis)guide cortical interneurons, we focally electroporated WT MGEs with *Ntn1* or *Unc5b* expression vectors. Overexpression of *Ntn1* had no obvious effect on interneuron migration when compared to the *GFP* control (Figures S7A–S7C). In contrast, using either a mouse or rat *Unc5b* construct, we found that *Unc5b* overexpression disrupted the migration of interneurons toward the cortex (m*Unc5b*: 16.2%, n = 11 versus *GFP*: 47.6%, n = 16 slices; p < 0.0001) (Figures 7E–7G, quantification in H; Figures S7A, S7B, and S7D). Interestingly, cells overproducing Unc5b tended to migrate in a ventral direction (Figure 7G).

As dependence receptor, Unc5b may also trigger cell death in absence of its ligand. We therefore investigated presence of cleaved caspase-3 as indicator of apoptosis in electroporated slices (Figures S7E and S7F). We did not observe a difference in cell death in *GFP* or *Unc5b* electroporated cells, suggesting that the migration defect induced by Unc5b overproduction is not a consequence of apoptosis. We also never observed increased cell death in the MGE of *Sip1* mutants (E14.5; data not shown).

If too high levels of Unc5b hamper the migration of *Sip1* KO interneurons, then we should be able to rescue their migration by downregulating *Unc5b*. We therefore electroporated Unc5b small interfering RNA (siRNA) or a nontargeting (NT) mouse siRNA pool in the MGE of Sip1|Nkx2-1 mutant slices. To visualize targeted *Sip1* KO cells, a conditional dsRed-expressing construct (pCALNL) was coelectroporated (Figure 7I). Electroporation of Unc5b siRNA almost doubled the number of *Sip1* mutant cells reaching the cortex (NT siRNA: 9.04%, n = 16 versus Unc5b siRNA: 13.82%, n = 11 slices; p < 0.0001) (Figures 7J and 7K, quantification in L). This indicates that decreasing the levels of endogenous Unc5b partially rescues the migration defect of *Sip1* KO interneurons.

In addition, we could also rescue the interneuron migration in vivo by using a Sip1 complementary DNA (cDNA)-encoded transgene conditionally expressed from the *ROSA* locus (R26-Sip1$^{tg/tg}$). This mouse delivers a relatively small but constant dose of Sip1 to cells that express Cre (M. Tatari and G. Berx, personal communication). Because the RCE reporter is also ROSA based, only hemizygous R26-Sip1 (R26-Sip1$^{tg/wt}$) samples could be obtained from FACS-sorted cells. Introduction of R26-Sip1$^{tg/wt}$ increased *Sip1* levels, while it reduced *Unc5b* levels in E14.5 *Sip1* KO cells, as measured by qPCR (representative samples shown in Figure 7D). Introduction of two R26-Sip1-based alleles (R26-Sip1$^{tg/tg}$) in a Sip1|Nkx2-1 KO mouse abolished the increase in *Unc5b* levels in the MGE (Figure 7C-C′) and rescued the migration of interneurons to the cortex, as seen at E16.5 (Figures 7M–7O and 7M′–7O′).

Altogether, our data show that Sip1 is needed for the proper regulation of the expression level of *Unc5b* in MGE-derived interneurons. Furthermore, our results also indicate that the local tuning of *Unc5b* expression in the MGE mantle zone is essential to direct the migratory path of these interneurons to the cortex.

DISCUSSION

In this study, we identify Sip1 as a critical, cell-autonomously acting transcription factor required in GABAergic interneurons, for their efficient migration to the cortex. Deletion of *Sip1* in the MGE results in misrouting of MGE-derived interneurons, indicating a guidance defect. Transcriptome analysis using RNA-seq followed by gain-of-function studies show that increased levels of Unc5b inhibit interneuron migration to the cortex.

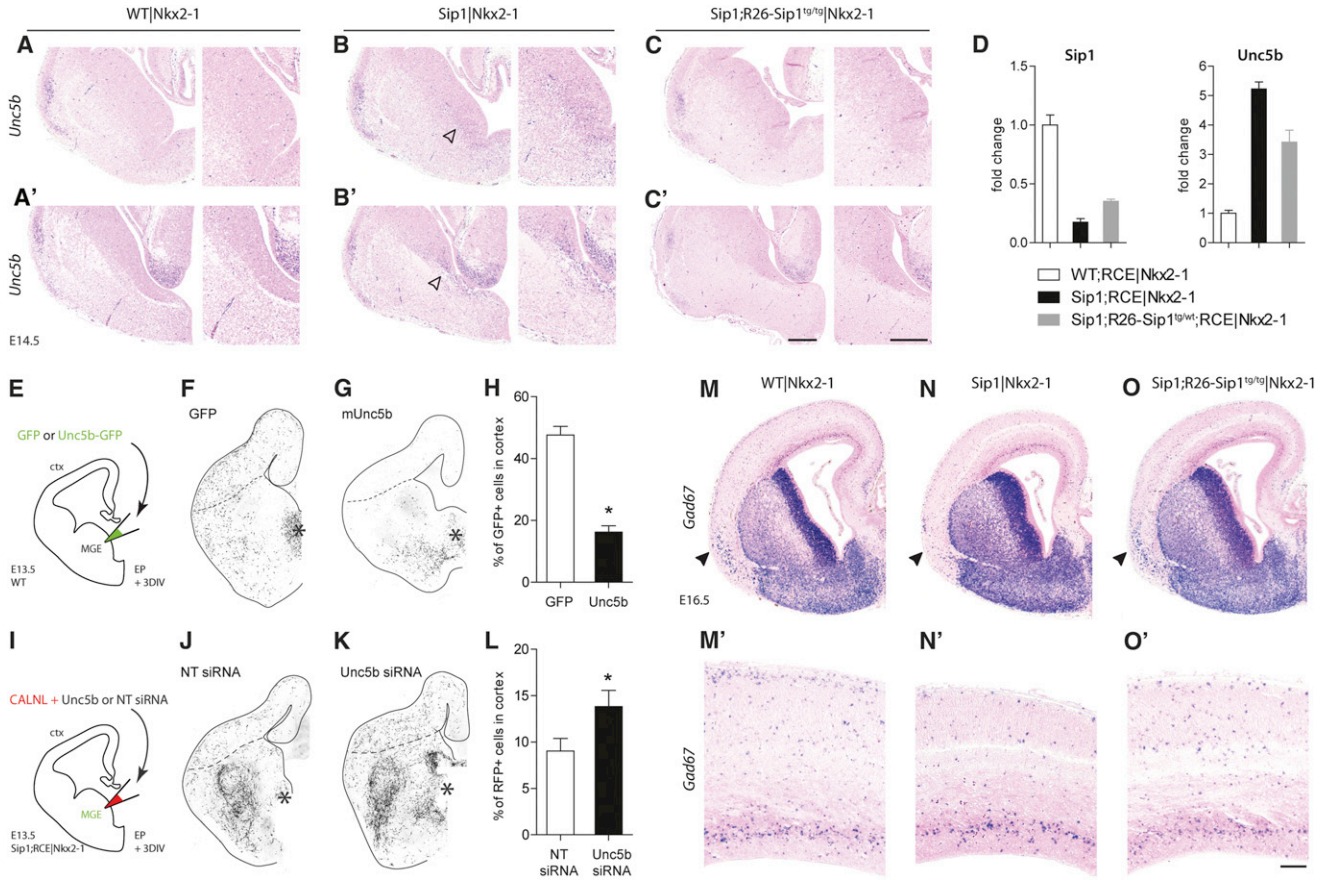

Figure 7. Tuning of Unc5b Levels Is Crucial for Directed Migration of MGE-Derived Cortical Interneurons

(A and B) In situ analysis in control and mutant brain sections reveals increased *Unc5b* levels in the Sip1|Nkx2-1 MGE (open arrowhead in B and B′)—rostral level (A and B); more caudal level (A′ and B′).

(C) *Unc5b* levels in the MGE were restored to base levels by crossing *Sip1* KO mice with a conditional *Sip1* transgenic mouse line, R26-Sip1$^{tg/tg}$ (C and C′). Same rostrocaudal levels shown as in (A, A′ and B, B′).

(D) Sip1 and Unc5b levels are inversely correlated, as shown by qPCR on representative E14.5 FACS-sorted control, KO and hemizygous rescue telencephalic samples (WT;RCE-, Sip1;RCE- and Sip1;R26-Sip1$^{tg/wt}$;RCE|Nkx2-1, respectively). qPCR was performed in duplicate, and error bars represent SD.

(E) Scheme of the focal electroporation experiment.

(F and G) Plasmids encoding GFP or Unc5b were focally electroporated in the MGE of WT E13.5 organotypic brain slices. After 3 DIV, many GFP+ interneurons were found in the cortex (F), whereas electroporation of mouse (m) Unc5b largely disrupted interneuron migration to the cortex (G).

(H) We calculated the percentage of GFP or mUnc5b interneurons in the cortex on the total amount of targeted cells per slice (GFP: 47.63% ± 2.78%, n = 16 slices versus mUnc5b: 16.22% ± 2.04%, n = 11 slices, $p < 0.0001$, χ^2 test). Error bars represent SEM, and n is the number of slices.

(I) Experimental design to rescue directed migration of *Sip1* KO interneurons.

(J and K) Nontargeting (NT) siRNA or mouse Unc5b siRNA was coelectroporated with a conditional dsRed-encoding plasmid (CALNL) to mark targeted cells in the Sip1;RCE|Nkx2-1 brain slices. After 3 DIV, almost no NT siRNA-treated *Sip1* KO cells were present in the cortex (J). Reducing Unc5b levels in Sip1;RCE|Nkx2-1 interneurons partially rescues the migration to the cortex (K).

(L) Quantification of the percentage of *Sip1* KO cells in the cortex upon NT or Unc5b siRNA electroporation (NT siRNA: 9.04% ± 1.36%, n = 16 slices versus Unc5b siRNA: 13.82% ± 1.76%, n = 16 slices, $p < 0.0001$, χ^2 test). Error bars represent SEM of two independent experiments, and n is the number of slices.

(M–O and M′–O′) Introduction of the R26-Sip1 transgene rescues the number of GABAergic interneuron in the *Sip1* KO cortex (higher magnifications in M′–O′ taken at the same level as indicated in Figure 2G). Rescue of migration to the cortex was also obvious in the piriform cortex (arrowheads).

Asterisks in (F) and (G) and (J) and (K) indicate the area of injection, and the dotted line indicates the border between cortex and VT. Scale bars in C′ represent 250 μm (A–C, A′–C′), and 100 μm in O′ (M′–O′).

See also Figures S5–S7.

Moreover, knockdown of Unc5b ex vivo in *Sip1* mutant brain slices or conditional expression of a *Sip1* transgene in vivo in a *Sip1* KO background rescue this phenotype. Hence, we identify Unc5b as a key Sip1-modulated guidance receptor in directed interneuron migration.

The *Sip1* mutant mice studied here recapitulate some features of MWS, in particular seizures, which are common in MWS patients (Garavelli and Mainardi, 2007). Defects in cortical interneuron migration typically cause seizures in mice (Powell et al., 2003; Levitt et al., 2004). In line with this, we observed

spontaneous seizures in Sip1|Gsh2 mutant mice during the third postnatal week, but not in young Sip1|Nkx2-1 mice, suggesting that *Sip1* deletion in CGE as well as MGE-derived interneurons (in Sip1|Gsh2 mice) is more detrimental than in the MGE alone (as in Sip1|Nkx2-1 mice).

Sip1 is produced in larger amounts by migrating interneurons than in progenitors, consistent with previous observations (Batista-Brito et al., 2008; Faux et al., 2010). Removal of *Sip1* from the entire CNS (Nestin-*Cre*) leads to a phenotype similar to that observed in Sip1|Dlx5/6 mice, in which VZ progenitors of the VT are not targeted, suggesting that Sip1 functions at the level of the SVZ and/or in postmitotic cells to drive differentiation. Similarly, during neural induction, as well as during mouse embryonic stem cell differentiation, Sip1 controls the formation of definitive neural stem cells from progenitor cells (van Grunsven et al., 2007; Dang et al., 2012). In embryonic hematopoiesis, Sip1 is also essential for stem/progenitor cell (HSC/HPC) differentiation and mobilization, but not for HSC formation itself (Goossens et al., 2011). Likewise, Sip1 promotes differentiation of oligodendrocyte precursor cells into myelinating cells (Weng et al., 2012).

Our transcriptome analysis shows that E14.5 *Sip1* KO cells have reduced levels of several cortical interneuron markers such as Cux2, Maf, Cxcr4, and Cxcr7, which may indicate a differentiation deficit. Persistent levels of Nkx2-1 in particular, instead of its downregulation in WT mice, may even suggest that these interneurons acquire a striatal or cholinergic fate. Unfortunately, at present, no other factors are known to be uniquely expressed in embryonic striatal interneurons, making a firm distinction between cortical or striatal interneuron fates based on transcriptome analysis rather difficult. It cannot be excluded that Sip1-deficient interneurons remain cortical in character but fail to differentiate fully, either because of the absence of Sip1 function(s) or rather because of a failure of these cells to be exposed to cortical maturation factors that allow them to articulate a fully mature cortical phenotype. Indeed, once in the neocortex, *Sip1* KO interneurons were able to contribute to the PV+ or SST+ cell populations.

Clearly, a large portion of *Sip1* KO cells never reach the cortex. Our unbiased GO analysis shows that axon guidance and cell adhesion factors were enriched among upregulated genes. In addition to other TFs, Sip1 is known to affect cell-cell adhesion in various contexts such as EMT and cancer, via direct regulation of *E-cadherin* expression. Because Sip1 directly represses *E-cadherin* (Comijn et al., 2001; van Grunsven et al., 2003) gain-of-function or high levels of Sip1 correlate with deadhesion, increased invasion, and bad prognosis in some cancers (Peinado et al., 2007), whereas loss-of-function of *Sip1* promotes adhesion and leads to delayed/reduced delamination of cranial neural crest cells (Van de Putte et al., 2003). Rather than possibly affecting cell-cell adhesion, our results show that *Sip1* deletion in interneurons deregulates their directed migration. During embryogenesis, an ectopic group of MGE-derived *Sip1* KO cells was found in the caudal VT. A comparable misrouting was described in the *Dlx1/2* double-mutant brain, accompanied with ectopia of cortical interneuron-like cells (Marín et al., 2001; Long et al., 2009).

Our data indicate that upregulation of Unc5b mRNA levels in interneurons results in their aberrant migration. Overexpression of *Unc5b* by focal electroporation in cells of the MGE indeed changes their direction of migration without influencing their differentiation into cortical interneurons, leading to a dramatic reduction in migration of interneurons to the cortex. Moreover, using a conditional overexpression approach, we show that *Sip1* levels are inversely correlated with *Unc5b* levels. On the other hand, Sip1 chromatin immunoprecipitation on conserved regions of the *Unc5b* upstream regulatory region and the first intron (100 kb around the transcription start site) did not detect any direct binding of Sip1, suggesting that Sip1 represses *Unc5b* expression indirectly (data not shown). Further work is needed to identify the Sip1 transcriptional target that directly represses *Unc5b*.

Which ligands could cause the misrouting of these Unc5b-overexpressing MGE cells? Ntn1 mediates repellent responses via Unc5b, alone or in combination with the receptor Dcc (Rajasekharan and Kennedy, 2009). Although Netrins have been implicated in cell and axon migration and Ntn1 is present along the migratory routes of GABAergic interneurons, the cortices of $Ntn1^{-/-}$ and $Slit1/2^{-/-};Ntn1^{-/-}$ mutants as well as $Dcc^{-/-}$ mutants display normal interneuron numbers at birth, suggesting that these proteins are dispensable for tangential migration (Anderson et al., 1999; Marín et al., 2003). However, Ntn1 interaction with $\alpha3\beta1$ integrin, which is present on interneurons, promotes their migration. Deletion of both *Ntn1* and *α3 integrin* (*Itga3*) results in a large ectopic aggregation of interneurons in the VT, suggesting that Ntn1 signaling provides directional information to migrating interneurons (Stanco et al., 2009). In addition to Ntn1, Unc5 receptors also bind Flrt2 and Flrt3, which results in a repellent interaction, based on observations with Unc5d and Flrt2 during radial migration of cortical projection neurons (Karaulanov et al., 2009; Yamagishi et al., 2011). We detect both *Flrt2 and Flrt3* in the LGE, a region through which MGE-derived interneurons migrate en route to the cortex. Moreover, *Ntn1* is present in the VZ of the LGE and MGE, as well as in the striatal anlage. High levels of Unc5b in interneurons could repel them from these Ntn- and Flrt-rich areas. Cells overexpressing *Unc5b* via focal electroporation preferentially migrate in a ventral direction, suggesting that they indeed avoid these Ntn1- and Flrt-rich areas. Further studies are necessary to define which ligand(s) is (are) primarily causing Sip1-deficient cells to deviate from their normal path in the VT.

In conclusion, our results identify Sip1 as an essential transcription factor for cortical interneuron migration and maturation. Furthermore, we demonstrate that the regulation of precise Unc5b levels by Sip1 represents a way of sorting the different MGE cell types generated during embryogenesis. In general, defining a global guidance code for each of the migrating cell types in the VT will be a challenge for the future.

EXPERIMENTAL PROCEDURES

Animals

Mice were maintained in a CD1/Swiss background and were kept at KU Leuven in accordance to Belgian and EU regulations. Mice carrying a floxed (exon 7) *Sip1* allele ($Sip1^{fl/fl}$) (Higashi et al., 2002) were crossed with the following *Cre* mouse lines: Nkx2-1-*Cre* and Gsh2-*Cre* (Kessaris et al., 2006), Nestin-*Cre* (Tronche et al., 1999), Dlx5/6-*Cre* (Stenman et al., 2003), with

RCE$^{fl/fl}$ reporter mice (Sousa et al., 2009) and conditional Sip1 transgenic ROSA26-Sip1$^{tg/tg}$ mice (M. Tatari and G. Berx, personal communication).

Immunohistochemistry and In Situ Hybridization

For the postnatal study, mice were deeply anesthetized with pentobarbital before intracardiac perfusion with MEMFA fixative. Brains were removed and fixed overnight, followed by progressive dehydration and paraffin embedding. Coronal and sagittal sections from embryonic brains were prepared as described (Seuntjens et al., 2009). Brain sections were processed for immunohistochemistry or in situ hybridization using an automated platform (Ventana Discovery, Roche). Antibodies and mRNA probes are listed in Supplemental Experimental Procedures. Sections were photographed using a Leica DMR microscope connected to a Spot camera (Visitron Systems). Three nonoverlapping pictures of 765 × 1,015 μm^2 were taken in the cortex from the lateral part of the cortex to the midline. The number of marker+, GFP+, and double GFP+/marker+ cells was quantified. Three animals (age P20–P24) were used for each genotype. Cells were counted via ImageJ software and results are represented as mean ± SD. Statistical significance was determined using the Student's t test.

MGE Explant Cultures in Matrigel

E14.5 WT;RCE|Nkx2-1 and Sip1;RCE|Nkx2-1 brains were dissected in ice-cold HEPES-buffered Leibovitz's L15 medium (Invitrogen) and embedded in 4% low-melting-point agarose. Organotypic slices of mouse telencephalon (coronal, 300 μm) were made using a vibratome (HM650V, Microm). MGE pieces were embedded in Matrigel on culture slides (both from BD Biosciences). Explants were cultured in Neurobasal/B27 medium for 1 or 2 DIV in a 5% CO_2-humidified incubator. Neurons that migrated the furthest away from the explants determined a circumference around the explant for which 15 to 20 radii were measured determining the average maximum migratory distance away from the explant. Statistical significance was determined via Mann-Whitney U test.

FACS of MGE-Derived Cells

E14.5 WT;RCE|-, Sip1;RCE|- and Sip1;R26-Sip1;RCE|Nkx2-1 telencephali were isolated in ice-cold HEPES-buffered Leibovitz's L15 medium (Invitrogen), meninges and olfactory lobes were removed and the tissue was cut in small pieces. Cells were dissociated by incubation in Papain solution (150 μl per brain of 12 U/ml) (Sigma) supplemented with DNaseI (30 U/ml) (Roche) for 30 min at 37°C followed by mechanical dispersion, washed with Dulbecco's PBS (Lonza) and passed over a 70 μm cell strainer (BD Falcon). Highly fluorescent cells (population P2) were sorted using a FACSVantage SE (FACSDiva) (BD Biosciences). Sorted cells were immediately lysed in TRIzol LS (Invitrogen) and RNA was extracted using the RNeasy Micro kit (QIAGEN).

RNA-Seq

RNA-seq library was prepared for analysis according to the Illumina TruSeq protocol (http://www.illumina.com). Briefly, poly(A)-tailed mRNA was copied into cDNA fragments, end repaired, (A)-tailed, ligated with adaptors, and enriched by PCR. Six RNA-seq library stocks were pooled and sequenced for 36 bp using the HiSeq 2000.

RNA-Seq Data Analysis

Three biological replicates of FACS-sorted WT;- and Sip1;RCE|Nkx2-1 samples were analyzed. The number of reads for the samples ranged from 13,737,422 to 17,967,187 (Table S4). Mapping was done with TopHat to the mouse reference genome (mm9) using default parameters (Trapnell et al., 2009), resulting in 79.03%–79.84% of uniquely mapped reads (Table S5). Read counts were aggregated for each gene using HT-Seq (http://www-huber.embl.de/users/anders/HTSeq/doc/overview.html) in the "union" mode (Ensembl r62 annotation). Gene expression levels were normalized using DE-Seq and filtered on a minimum of 150.0 normalized read count in at least one condition. Differential expression analysis was performed with DE-Seq (FDR < 0.05), resulting in 505 genes significantly upregulated and 366 genes significantly downregulated in Sip1;RCE|Nkx2-1, compared to control. GO enrichment was performed using GOrilla on a single ranked list (http://cbl-gorilla.cs.technion.ac.il).

qPCR

RNA was obtained from FACS-sorted E14.5 WT;RCE|-, Sip1;RCE|-, and Sip1;R26-Sip1;RCE|Nkx2-1 telencephalic cells and cDNA was made via the SuperScript III First-Strand Synthesis System (Invitrogen). qPCR was carried out in duplicate on a LightCycler 480 Instrument (Roche) using SYBR Green PCR Master Mix (Roche). Relative quantitation was determined using qBasePLUS software.

Plasmids

Expression constructs used for focal electroporation were based on pCIG, a pCAGGS-IRES-*eGFP* plasmid obtained via P. Vanderhaeghen (Megason and McMahon, 2002). In the multiple cloning site of this vector, we cloned (1) the mouse Unc5b coding sequence which was isolated from a pcDNA3-*mUnc5b* construct (Yamagishi et al., 2011), (2) the rat Unc5b-coding sequence isolated from the pEGFP-N1/*rUnc5b* construct (Larrivée et al., 2007), and (3) the mouse Netrin1 coding sequence isolated from a *Ntn1* expression plasmid (IRCKp5014G0516Q, ImaGenes). To trace electroporated cells in RCE|Nkx2-1 brain slices, the pCALNL plasmid (Addgene) was used. To delete *Sip1* in *Sip1*$^{fl/fl}$ brain slices, a pCIG-*Cre* plasmid was used (P. Vanderhaeghen).

Focal Electroporation

Focal electroporation of MGEs from E13.5 WT, *Sip1*$^{fl/fl}$, or Sip1;RCE|Nkx2-1 embryos was done as described previously (Passante et al., 2008) and carried out with the aforementioned plasmids at 1 μg/μl and 4% fast green (Sigma). For overexpression, pCIG-mUnc5b was mixed in a 1:1 ratio with pCIG (0.5 μg/μl) and 1 μg/μl was used for the pCIG-*rUnc5b* construct. To rescue the migration of *Sip1* KO interneurons, mouse Unc5b siRNAs (Smartpool, ON-TARGET plus, Thermo Scientific) or a NT pool of mouse siRNAs were used (200 μM) and mixed with pCALNL plasmid (1 μg/μl) to trace the electroporated cells. Electroporated slices were cultured for 3 DIV using an air-interface protocol (Polleux and Ghosh, 2002). Slices were fixed with 4% paraformaldehyde and analyzed via confocal microscopy (Nikon A1R Eclipse Ti). For each condition, we quantified (via ImageJ software) the total amount of GFP+ or RFP+ cells in the slice and calculated the percentage of GFP+ or RFP+ neurons that reached the cortex. Statistical significance was determined using the χ^2 test.

Immunohistochemistry in Electroporated Slices

Slices were preincubated for 1 hr with PBS containing 0.3% triton (PBST) and 10% normal donkey serum. Primary antibodies (rabbit anti-cleaved caspase-3, 1:500, Cell Signaling Technologies; goat anti-GFP, 1:200, Abcam) were added overnight at 4°C. After washes in PBST, secondary antibodies (donkey anti-rabbit CY3 and donkey anti-goat Dylight 488, both at 1:1,000, Jackson ImmunoResearch) were applied overnight at 4°C. Slices were washed in PBST and mounted in Mowiol, and pictures were taken with a Nikon A1R Eclipse Ti confocal microscope.

ACCESSION NUMBERS

Data sets have been deposited in the GEO under the accession number GSE35616 (http://www.ncbi.nlm.nih.gov/geo/query/acc.cgi?acc=GSE35616).

SUPPLEMENTAL INFORMATION

Supplemental Information includes seven figures, seven tables, and Supplemental Experimental Procedures and can be found with this article online at http://dx.doi.org/10.1016/j.neuron.2012.11.009.

ACKNOWLEDGMENTS

We thank K. Campbell and R. Klein for sharing mouse lines. We also thank D.J. Anderson, C. Birchmeier, K. Campbell, B. Condie, J. Egea, A. Eichmann, Z. Kaprielian, R. Klein, and M. Price for sharing plasmids and reagents, V. Van Duppen for FACS-sorting, and A. van der Sloot for RNA sequencing. We appreciate the advice of A. Gaertner and all members of the A. Zwijsen and DH labs, and H. Kondoh and Y. Higashi for previous important contributions.

This work was funded by the Research Council of KU Leuven (OT-09/053 and GOA-11/012, to D.H.), FWO-V (G.0954.11N, to D.H. and E. Seuntjens), the Queen Elisabeth Medical Foundation (to P.V.; and GSKE 1113, to D.H. and E. Seuntjens), the Interuniversity Attraction Poles (IUAP-VI/20 funding to D.H., A.G., and P.V., and IUAP-VII/07 funding to D.H.), the InfraMouse Grant from the Hercules Foundation (ZW09-03, to D.H.), the visiting professor program from the Royal Netherlands Academy of Arts and Sciences (to D.H.), and the intercommunity visiting program of the Francqui Foundation (to E. Seuntjens and A.G.). The N.K. lab is funded by the European Research Council (ERC-STG 207807) and the Wellcome Trust. Work from P.V. was supported by the Action de Recherches Concertées (ARC) Programs of the Communauté Wallonie/Bruxelles, the Federal Office for Scientific, Technical and Cultural Affairs, the FNRS, and Welbio and Programme d'Excellence CIBLES of the Walloon Region. P.V. is a FNRS Research Director, J.D. was a FRIA Research Fellow, and S.G. is supported by FWO. V.vdB., E. Stappers, and R.D. are supported by the Agency for Innovation by Science and Technology (IWT).

Accepted: November 4, 2012
Published: January 9, 2013

REFERENCES

Anders, S., and Huber, W. (2010). Differential expression analysis for sequence count data. Genome Biol. *11*, R106.

Anderson, S., Mione, M., Yun, K., and Rubenstein, J.L. (1999). Differential origins of neocortical projection and local circuit neurons: role of Dlx genes in neocortical interneuronogenesis. Cereb. Cortex *9*, 646–654.

Andrews, W., Liapi, A., Plachez, C., Camurri, L., Zhang, J., Mori, S., Murakami, F., Parnavelas, J.G., Sundaresan, V., and Richards, L.J. (2006). Robo1 regulates the development of major axon tracts and interneuron migration in the forebrain. Development *133*, 2243–2252.

Andrews, W., Barber, M., Hernadez-Miranda, L.R., Xian, J., Rakic, S., Sundaresan, V., Rabbitts, T.H., Pannell, R., Rabbitts, P., Thompson, H., et al. (2008). The role of Slit-Robo signaling in the generation, migration and morphological differentiation of cortical interneurons. Dev. Biol. *313*, 648–658.

Ascoli, G.A., Alonso-Nanclares, L., Anderson, S.A., Barrionuevo, G., Benavides-Piccione, R., Burkhalter, A., Buzsáki, G., Cauli, B., Defelipe, J., Fairén, A., et al.; Petilla Interneuron Nomenclature Group. (2008). Petilla terminology: nomenclature of features of GABAergic interneurons of the cerebral cortex. Nat. Rev. Neurosci. *9*, 557–568.

Batista-Brito, R., Machold, R., Klein, C., and Fishell, G. (2008). Gene expression in cortical interneuron precursors is prescient of their mature function. Cereb. Cortex *18*, 2306–2317.

Chédotal, A., and Rijli, F.M. (2009). Transcriptional regulation of tangential neuronal migration in the developing forebrain. Curr. Opin. Neurobiol. *19*, 139–145.

Comijn, J., Berx, G., Vermassen, P., Verschueren, K., van Grunsven, L., Bruyneel, E., Mareel, M., Huylebroeck, D., and van Roy, F. (2001). The two-handed E box binding zinc finger protein SIP1 downregulates E-cadherin and induces invasion. Mol. Cell *7*, 1267–1278.

Conidi, A., Cazzola, S., Beets, K., Coddens, K., Collart, C., Cornelis, F., Cox, L., Joke, D., Dobreva, M.P., Dries, R., et al. (2011). Few Smad proteins and many Smad-interacting proteins yield multiple functions and action modes in TGFβ/BMP signaling in vivo. Cytokine Growth Factor Rev. *22*, 287–300.

Corbin, J.G., and Butt, S.J. (2011). Developmental mechanisms for the generation of telencephalic interneurons. Dev. Neurobiol. *71*, 710–732.

Dang, L.T., Wong, L., and Tropepe, V. (2012). Zfhx1b induces a definitive neural stem cell fate in mouse embryonic stem cells. Stem Cells Dev. *21*, 2838–2851.

Faux, C., Rakic, S., Andrews, W., Yanagawa, Y., Obata, K., and Parnavelas, J.G. (2010). Differential gene expression in migrating cortical interneurons during mouse forebrain development. J. Comp. Neurol. *518*, 1232–1248.

Flames, N., Long, J.E., Garratt, A.N., Fischer, T.M., Gassmann, M., Birchmeier, C., Lai, C., Rubenstein, J.L., and Marín, O. (2004). Short- and long-range attraction of cortical GABAergic interneurons by neuregulin-1. Neuron *44*, 251–261.

Fogarty, M., Grist, M., Gelman, D., Marín, O., Pachnis, V., and Kessaris, N. (2007). Spatial genetic patterning of the embryonic neuroepithelium generates GABAergic interneuron diversity in the adult cortex. J. Neurosci. *27*, 10935–10946.

Garavelli, L., and Mainardi, P.C. (2007). Mowat-Wilson syndrome. Orphanet J. Rare Dis. *2*, 42.

Gelman, D.M., Martini, F.J., Nóbrega-Pereira, S., Pierani, A., Kessaris, N., and Marín, O. (2009). The embryonic preoptic area is a novel source of cortical GABAergic interneurons. J. Neurosci. *29*, 9380–9389.

Goossens, S., Janzen, V., Bartunkova, S., Yokomizo, T., Drogat, B., Crisan, M., Haigh, K., Seuntjens, E., Umans, L., Riedt, T., et al. (2011). The EMT regulator Zeb2/Sip1 is essential for murine embryonic hematopoietic stem/progenitor cell differentiation and mobilization. Blood *117*, 5620–5630.

Hernández-Miranda, L.R., Cariboni, A., Faux, C., Ruhrberg, C., Cho, J.H., Cloutier, J.F., Eickholt, B.J., Parnavelas, J.G., and Andrews, W.D. (2011). Robo1 regulates semaphorin signaling to guide the migration of cortical interneurons through the ventral forebrain. J. Neurosci. *31*, 6174–6187.

Higashi, Y., Maruhashi, M., Nelles, L., Van de Putte, T., Verschueren, K., Miyoshi, T., Yoshimoto, A., Kondoh, H., and Huylebroeck, D. (2002). Generation of the floxed allele of the SIP1 (Smad-interacting protein 1) gene for Cre-mediated conditional knockout in the mouse. Genesis *32*, 82–84.

Karaulanov, E., Böttcher, R.T., Stannek, P., Wu, W., Rau, M., Ogata, S., Cho, K.W., and Niehrs, C. (2009). Unc5B interacts with FLRT3 and Rnd1 to modulate cell adhesion in Xenopus embryos. PLoS ONE *4*, e5742.

Kessaris, N., Fogarty, M., Iannarelli, P., Grist, M., Wegner, M., and Richardson, W.D. (2006). Competing waves of oligodendrocytes in the forebrain and postnatal elimination of an embryonic lineage. Nat. Neurosci. *9*, 173–179.

Larrivée, B., Freitas, C., Trombe, M., Lv, X., Delafarge, B., Yuan, L., Bouvrée, K., Bréant, C., Del Toro, R., Bréchot, N., et al. (2007). Activation of the UNC5B receptor by Netrin-1 inhibits sprouting angiogenesis. Genes Dev. *21*, 2433–2447.

Levitt, P., Eagleson, K.L., and Powell, E.M. (2004). Regulation of neocortical interneuron development and the implications for neurodevelopmental disorders. Trends Neurosci. *27*, 400–406.

Li, G., Adesnik, H., Li, J., Long, J., Nicoll, R.A., Rubenstein, J.L., and Pleasure, S.J. (2008). Regional distribution of cortical interneurons and development of inhibitory tone are regulated by Cxcl12/Cxcr4 signaling. J. Neurosci. *28*, 1085–1098.

Long, J.E., Cobos, I., Potter, G.B., and Rubenstein, J.L. (2009). Dlx1&2 and Mash1 transcription factors control MGE and CGE patterning and differentiation through parallel and overlapping pathways. Cereb. Cortex *19*(*Suppl 1*), i96–i106.

López-Bendito, G., Sánchez-Alcañiz, J.A., Pla, R., Borrell, V., Picó, E., Valdeolmillos, M., and Marín, O. (2008). Chemokine signaling controls intracortical migration and final distribution of GABAergic interneurons. J. Neurosci. *28*, 1613–1624.

Marín, O., Yaron, A., Bagri, A., Tessier-Lavigne, M., and Rubenstein, J.L. (2001). Sorting of striatal and cortical interneurons regulated by semaphorin-neuropilin interactions. Science *293*, 872–875.

Marín, O., Plump, A.S., Flames, N., Sánchez-Camacho, C., Tessier-Lavigne, M., and Rubenstein, J.L. (2003). Directional guidance of interneuron migration to the cerebral cortex relies on subcortical Slit1/2-independent repulsion and cortical attraction. Development *130*, 1889–1901.

Markram, H., Toledo-Rodriguez, M., Wang, Y., Gupta, A., Silberberg, G., and Wu, C. (2004). Interneurons of the neocortical inhibitory system. Nat. Rev. Neurosci. *5*, 793–807.

Marsh, E.D., Minarcik, J., Campbell, K., Brooks-Kayal, A.R., and Golden, J.A. (2008). FACS-array gene expression analysis during early development of mouse telencephalic interneurons. Dev. Neurobiol. *68*, 434–445.

Megason, S.G., and McMahon, A.P. (2002). A mitogen gradient of dorsal midline Wnts organizes growth in the CNS. Development *129*, 2087–2098.

Miquelajauregui, A., Van de Putte, T., Polyakov, A., Nityanandam, A., Boppana, S., Seuntjens, E., Karabinos, A., Higashi, Y., Huylebroeck, D., and Tarabykin, V. (2007). Smad-interacting protein-1 (Zfhx1b) acts upstream of Wnt signaling in the mouse hippocampus and controls its formation. Proc. Natl. Acad. Sci. USA *104*, 12919–12924.

Miyoshi, G., Butt, S.J.B., Takebayashi, H., and Fishell, G. (2007). Physiologically distinct temporal cohorts of cortical interneurons arise from telencephalic Olig2-expressing precursors. J. Neurosci. *27*, 7786–7798.

Miyoshi, G., Hjerling-Leffler, J., Karayannis, T., Sousa, V.H., Butt, S.J., Battiste, J., Johnson, J.E., Machold, R.P., and Fishell, G. (2010). Genetic fate mapping reveals that the caudal ganglionic eminence produces a large and diverse population of superficial cortical interneurons. J. Neurosci. *30*, 1582–1594.

Nóbrega-Pereira, S., Kessaris, N., Du, T., Kimura, S., Anderson, S.A., and Marín, O. (2008). Postmitotic Nkx2-1 controls the migration of telencephalic interneurons by direct repression of guidance receptors. Neuron *59*, 733–745.

Passante, L., Gaspard, N., Degraeve, M., Frisén, J., Kullander, K., De Maertelaer, V., and Vanderhaeghen, P. (2008). Temporal regulation of ephrin/Eph signalling is required for the spatial patterning of the mammalian striatum. Development *135*, 3281–3290.

Peinado, H., Olmeda, D., and Cano, A. (2007). Snail, Zeb and bHLH factors in tumour progression: an alliance against the epithelial phenotype? Nat. Rev. Cancer *7*, 415–428.

Polleux, F., and Ghosh, A. (2002). The slice overlay assay: a versatile tool to study the influence of extracellular signals on neuronal development. Sci. STKE *2002*, pl9.

Powell, E.M., Campbell, D.B., Stanwood, G.D., Davis, C., Noebels, J.L., and Levitt, P. (2003). Genetic disruption of cortical interneuron development causes region- and GABA cell type-specific deficits, epilepsy, and behavioral dysfunction. J. Neurosci. *23*, 622–631.

Rajasekharan, S., and Kennedy, T.E. (2009). The netrin protein family. Genome Biol. *10*, 239.

Rubin, A.N., Alfonsi, F., Humphreys, M.P., Choi, C.K., Rocha, S.F., and Kessaris, N. (2010). The germinal zones of the basal ganglia but not the septum generate GABAergic interneurons for the cortex. J. Neurosci. *30*, 12050–12062.

Rudolph, J., Zimmer, G., Steinecke, A., Barchmann, S., and Bolz, J. (2010). Ephrins guide migrating cortical interneurons in the basal telencephalon. Cell Adhes. Migr. *4*, 400–408.

Sánchez-Alcañiz, J.A., Haege, S., Mueller, W., Pla, R., Mackay, F., Schulz, S., López-Bendito, G., Stumm, R., and Marín, O. (2011). Cxcr7 controls neuronal migration by regulating chemokine responsiveness. Neuron *69*, 77–90.

Seuntjens, E., Nityanandam, A., Miquelajauregui, A., Debruyn, J., Stryjewska, A., Goebbels, S., Nave, K.A., Huylebroeck, D., and Tarabykin, V. (2009). Sip1 regulates sequential fate decisions by feedback signaling from postmitotic neurons to progenitors. Nat. Neurosci. *12*, 1373–1380.

Sousa, V.H., Miyoshi, G., Hjerling-Leffler, J., Karayannis, T., and Fishell, G. (2009). Characterization of Nkx6-2-derived neocortical interneuron lineages. Cereb. Cortex *19*(*Suppl 1*), i1–i10.

Stanco, A., Szekeres, C., Patel, N., Rao, S., Campbell, K., Kreidberg, J.A., Polleux, F., and Anton, E.S. (2009). Netrin-1-alpha3beta1 integrin interactions regulate the migration of interneurons through the cortical marginal zone. Proc. Natl. Acad. Sci. USA *106*, 7595–7600.

Stenman, J., Toresson, H., and Campbell, K. (2003). Identification of two distinct progenitor populations in the lateral ganglionic eminence: implications for striatal and olfactory bulb neurogenesis. J. Neurosci. *23*, 167–174.

Stumm, R.K., Zhou, C., Ara, T., Lazarini, F., Dubois-Dalcq, M., Nagasawa, T., Höllt, V., and Schulz, S. (2003). CXCR4 regulates interneuron migration in the developing neocortex. J. Neurosci. *23*, 5123–5130.

Trapnell, C., Pachter, L., and Salzberg, S.L. (2009). TopHat: discovering splice junctions with RNA-Seq. Bioinformatics *25*, 1105–1111.

Tronche, F., Kellendonk, C., Kretz, O., Gass, P., Anlag, K., Orban, P.C., Bock, R., Klein, R., and Schütz, G. (1999). Disruption of the glucocorticoid receptor gene in the nervous system results in reduced anxiety. Nat. Genet. *23*, 99–103.

Van de Putte, T., Maruhashi, M., Francis, A., Nelles, L., Kondoh, H., Huylebroeck, D., and Higashi, Y. (2003). Mice lacking ZFHX1B, the gene that codes for Smad-interacting protein-1, reveal a role for multiple neural crest cell defects in the etiology of Hirschsprung disease-mental retardation syndrome. Am. J. Hum. Genet. *72*, 465–470.

van Grunsven, L.A., Michiels, C., Van de Putte, T., Nelles, L., Wuytens, G., Verschueren, K., and Huylebroeck, D. (2003). Interaction between Smad-interacting protein-1 and the corepressor C-terminal binding protein is dispensable for transcriptional repression of E-cadherin. J. Biol. Chem. *278*, 26135–26145.

van Grunsven, L.A., Taelman, V., Michiels, C., Verstappen, G., Souopgui, J., Nichane, M., Moens, E., Opdecamp, K., Vanhomwegen, J., Kricha, S., et al. (2007). XSip1 neuralizing activity involves the co-repressor CtBP and occurs through BMP dependent and independent mechanisms. Dev. Biol. *306*, 34–49.

Verschueren, K., Remacle, J.E., Collart, C., Kraft, H., Baker, B.S., Tylzanowski, P., Nelles, L., Wuytens, G., Su, M.T., Bodmer, R., et al. (1999). SIP1, a novel zinc finger/homeodomain repressor, interacts with Smad proteins and binds to 5′-CACCT sequences in candidate target genes. J. Biol. Chem. *274*, 20489–20498.

Verstappen, G., van Grunsven, L.A., Michiels, C., Van de Putte, T., Souopgui, J., Van Damme, J., Bellefroid, E., Vandekerckhove, J., and Huylebroeck, D. (2008). Atypical Mowat-Wilson patient confirms the importance of the novel association between ZFHX1B/SIP1 and NuRD corepressor complex. Hum. Mol. Genet. *17*, 1175–1183.

Wang, Y., Li, G., Stanco, A., Long, J.E., Crawford, D., Potter, G.B., Pleasure, S.J., Behrens, T., and Rubenstein, J.L. (2011). CXCR4 and CXCR7 have distinct functions in regulating interneuron migration. Neuron *69*, 61–76.

Weng, Q., Chen, Y., Wang, H., Xu, X., Yang, B., He, Q., Shou, W., Chen, Y., Higashi, Y., van den Berghe, V., et al. (2012). Dual-mode modulation of Smad signaling by Smad-interacting protein Sip1 is required for myelination in the central nervous system. Neuron *73*, 713–728.

Wichterle, H., Garcia-Verdugo, J.M., Herrera, D.G., and Alvarez-Buylla, A. (1999). Young neurons from medial ganglionic eminence disperse in adult and embryonic brain. Nat. Neurosci. *2*, 461–466.

Xu, Q., Tam, M., and Anderson, S.A. (2008). Fate mapping Nkx2.1-lineage cells in the mouse telencephalon. J. Comp. Neurol. *506*, 16–29.

Yamagishi, S., Hampel, F., Hata, K., Del Toro, D., Schwark, M., Kvachnina, E., Bastmeyer, M., Yamashita, T., Tarabykin, V., Klein, R., and Egea, J. (2011). FLRT2 and FLRT3 act as repulsive guidance cues for Unc5-positive neurons. EMBO J. *30*, 2920–2933.

Zimmer, G., Garcez, P., Rudolph, J., Niehage, R., Weth, F., Lent, R., and Bolz, J. (2008). Ephrin-A5 acts as a repulsive cue for migrating cortical interneurons. Eur. J. Neurosci. *28*, 62–73.

Zweier, C., Albrecht, B., Mitulla, B., Behrens, R., Beese, M., Gillessen-Kaesbach, G., Rott, H.D., and Rauch, A. (2002). "Mowat-Wilson" syndrome with and without Hirschsprung disease is a distinct, recognizable multiple congenital anomalies-mental retardation syndrome caused by mutations in the zinc finger homeo box 1B gene. Am. J. Med. Genet. *108*, 177–181.